Università di Catania

DIPARTIMENTO DI FISICA E ASTRONOMIA
"ETTORE MAJORANA"
UFFICIO PROVVEDITORALE E SERVIZI M.E.P.A.
UFFICIO ECONOMALE E SERVIZI M.E.P.A.

ATTO DI LIQUIDAZIONE

IL DIRETTORE

vista la legge n. 168/89 e ss.mm.ii.;

visto il D. Lgs. n. 165/2001 e ss.mm.ii.;

visto lo Statuto dell'Università degli Studi di Catania, emanato con D.R. n. 881 del 23 marzo 2015 e ss.mm.ii.;

visto il Regolamento di Ateneo per l'Amministrazione, la Contabilità e la Finanza, emanato con D.R. n. 9 del 04.01.2016 e ss.mm.ii.;

visto il D. Lgs. n. 50 del 18 aprile 2016 e ss.mm.ii.;

viste le deliberazioni del Consiglio di Amministrazione relative alla macro-organizzazione dell'Ateneo e in particolare quella del 30/06/2022 che introduce alcune modifiche organizzative al fine di razionalizzare l'impiego del personale e di migliorare l'efficienza dei servizi resi;

visto il Regolamento in materia di affidamento di lavori, beni e servizi per importi inferiori alla soglia comunitaria, emanato con D.R. rep. 2277 del 05/07/2022;

visto il buono d'ordine n. 69 del 21/10/2025 avente ad oggetto la fornitura di un servizio di pubblicazione scientifica per l'importo complessivo di € 2.445,00;

vista l'invoice della SPRINGER NATURE CUSTOMER SERVICE CENTER GMBH n. 2936578900 del 04/08/2025 dell'importo di € 2.445,00;

vista la prenotazione di budget n. 97404;

TRASMETTE

ai servizi finanziari la documentazione affinché provveda ad emettere BONIFICO ESTERO di € 2.445,00 a titolo di imponibile, per attività istituzionale, a favore dell'impresa SPRINGER NATURE CUSTOMER SERVICE CENTER GMBH avente sede legale in Europaplatz 3 99146 Heidelberg (GERMANIA) a saldo dell'invoice n. 2936578900 del 04/08/2025 richiamata in premessa, da accreditare sul conto IBAN DE22 7002 0270 0654 793298 BIC HYVEDEMMXXX fermi restando i controlli di carattere amministrativo, contabile e fiscale di competenza dei servizi finanziari previsti dalla normativa vigente.

Catania,

Il Direttore del DFA
Prof. Stefano Romano

INTEGRAZIONE FATTURA

N.: 2936578900

Del: 04/08/2025

FISICA ED ASTRONOMIA (DFA)

Fornitore

SPRINGER NATURE CUSTOMER SERVICE CENTEI GMBH
Europaplatz 3
99146 69115 HEIDELBERG

GERMANIA

Riferimento: INVOICE 2936578900 DEL 04/08/2025

Altri Dati Fornitore :
P.I. DE209719094

Attività istituzionale

N.I. 243 - PUBBLICAZ. SCIENTIFICA PROF. MIRABELLA

Natura della transazione	Paese di provenienza	Paese di origine	Provincia di destinazione	Paese di pagamento
Transazioni che comportano un effettivo trasferimento della proprietà dietro corrispettivo finanziario	DE Germania	DE Germania	Catania	DE Germania
Modalità di Pagamento	Valuta	Tasso di Cambio		
Bonifico				

Descrizione - Tipo IVA	Imponibile Totale in Valuta	Imponibile Totale EUR	Non Imp./ Esente EUR	Iva (%)	Importo Iva	Importo Totale EUR
PUBBLICAZ. SCIENTIFICA PROF. MIRABELLA IVA 22% servizi INTRA UE istituzionali		€ 2.445,00		22,00 %	€ 537,90	€ 2.982,90
Tipologia VF24		Descrizione Servizio				Modalità di Erogazione
		58142 Giornali e pubblicazioni periodiche on line				Istantanea

Totale Imponibile in Valuta	Totale Imponibile EUR	Totale Esente EUR	Iva	Totale documento
	€ 2.445,00		**€ 537,90**	**€ 2,982.90**

21/10/2025

Oggetto: Determina per l'affidamento diretto della fornitura di un servizio di pubblicazione scientifica ai sensi dell'art. 50 co. 1 lett. B) del D.L.vo 31 marzo 2023 n. 36, per un importo contrattuale pari a € 2.445,00 (IVA esclusa), CIG: B8B53AD753 – CUP E53D23016050001

IL DIRETTORE DEL DIPARTIMENTO

DI FISICA E ASTRONOMIA "ETTORE MAJORANA"

VISTO il R.D. 18 novembre 1923, n. 2440, recante "Nuove disposizioni sull'amministrazione del Patrimonio e la Contabilità Generale dello Stato";

VISTA la L. 7 agosto 1990, n. 241, recante «Nuove norme sul procedimento amministrativo»;

VISTO il D.Lgs. 31 marzo 2023, n. 36, recante «Codice dei contratti pubblici»;

VISTO lo Statuto dell'Università degli Studi di Catania, emanato con D.R. n. 881 del 23 marzo 2015 e ss.mm.;

VISTO il Regolamento per l'amministrazione, la contabilità e la finanza, emanato con D.R. n. 9 del 4 gennaio 2016 e ss.mm.;

VISTO il Regolamento dell'Università degli Studi di Catania in materia di affidamenti di lavori, beni e servizi per importi inferiori alle soglie di rilevanza comunitaria, emanato con D.R. 2277 del 05/07/2022 e ss. mm.;

VISTO il D.L. 16 luglio 2020, n. 76, convertito in L. 11 settembre 2020, n. 120, recante «Misure urgenti per la semplificazione e l'innovazione digitale»;

VISTO l'art. 50 co. 1 lett. b) del D.L.vo 31 marzo 2023 n. 36, ai sensi del quale "Salvo quanto previsto dagli articoli 62 e 63, le stazioni appaltanti procedono all'affidamento dei contratti di lavori, servizi e forniture di importo inferiore alle soglie di cui all'articolo 14 con le seguenti modalità:... b) affidamento diretto dei servizi e forniture, ivi compresi i servizi di ingegneria e architettura e l'attività di progettazione, di importo inferiore a 140.000 euro, anche senza consultazione di più operatori economici, assicurando che siano scelti soggetti in possesso di documentate esperienze pregresse idonee all'esecuzione delle prestazioni contrattuali, anche individuati tra gli iscritti in elenchi o albi istituiti dalla stazione appaltante";

VISTO l'art. 1, comma 449, della L. 27 dicembre 2006, n. 296, come modificato dall'art. 1, comma 495 della L. n. 28 dicembre 2015, n. 208, il quale prevede che tutte le amministrazioni statali centrali e periferiche, ivi comprese le scuole di ogni ordine e grado, sono tenute ad approvvigionarsi utilizzando le convenzioni stipulate da Consip S.p.A.;

VISTO l'art. 1, comma 583, della L. 27 dicembre 2019, n. 160, ai sensi del quale, fermo restando quanto previsto dal succitato art. 1, comma 449 e 450, della L. 296/2006, le amministrazioni statali centrali e periferiche, ivi compresi gli istituti e le scuole di ogni ordine e grado, sono tenute ad approvvigionarsi

attraverso gli accordi quadro stipulati da Consip S.p.A. o il Sistema Dinamico di Acquisizione (SDAPA) realizzato e gestito da Consip S.p.A.;

DATO ATTO della non esistenza di Convenzioni Consip attive in merito a tale merceologia;

VISTO l'art. 15, comma 1, del D.Lgs. 36/2023, il quale prevede l'individuazione di un responsabile unico del procedimento (RUP) per ogni singola procedura di affidamento;

VISTO l'Allegato I.2 al D.Lgs. 36/2023, recante «Attività del RUP»;

RITENUTO che il Sig. Nunzio Giudice risulta pienamente idoneo a ricoprire l'incarico di RUP per l'affidamento in oggetto, in quanto soddisfa i requisiti richiesti dall'art. 15, comma 2, del D.Lgs. 36/2023 e dall'art. 3 dell'Allegato I.2 al D.Lgs. 36/2023;

VISTO l'art. 6 bis della L. 241/90, relativo all'obbligo di astensione dall'incarico del responsabile del procedimento in caso di conflitto di interessi, e all'obbligo di segnalazione da parte dello stesso di ogni situazione di conflitto (anche potenziale);

VISTO altresì l'art. 16 comma 3 del D.Lgs. 36/2023, recante «Individuazione e gestione dei conflitti di interesse nelle procedure di affidamento di contratti pubblici»;

TENUTO CONTO che, nei confronti del RUP individuato non sussistono le condizioni ostative previste dalla succitata norma;

CONSIDERATO che, nel procedere all'acquisizione dei preventivi di spesa, il R.U.P. ha consultato la ditta **SPRINGER NATURE CUSTOMER SERVICE CENTER GMBH** ;

CONSIDERATO che l'operatore **SPRINGER NATURE CUSTOMER SERVICE CENTER GMBH** ha presentato un preventivo congruo e rientrante nella disponibilità del Dipartimento;

RITENUTO di procedere all'affidamento in oggetto in favore del suddetto operatore;

TENUTO CONTO che l'affidamento in oggetto dà luogo ad una transazione soggetta agli obblighi di tracciabilità dei flussi finanziari previsti dalla L. 13 agosto 2010, n. 136 e dal D.L. 12 novembre 2010, n. 187;

CONSIDERATO che gli importi di cui al presente provvedimento, trovano copertura finanziaria nel bilancio di previsione;

nell'osservanza delle disposizioni di cui alla L. 6 novembre 2012, n. 190, recante «Disposizioni per la prevenzione e la repressione della corruzione e dell'illegalità della Pubblica Amministrazione»,

DETERMINA

Per i motivi espressi nella premessa, che si intendono integralmente richiamati:

- di autorizzare, ai sensi dell'art. 1, comma 2, lettera a), del D.L. 76/2020, come modificato dal D.L. 77/2021, convertito nella Legge n. 108/2021, l'affidamento diretto della fornitura in oggetto all'operatore economico **SPRINGER NATURE CUSTOMER SERVICE CENTER GMBH** per un importo complessivo delle prestazioni pari ad € 2.445,00 omnicomprensivo;
- di autorizzare la spesa complessiva € 2.445,00 da imputare sulla prenotazione di budget n. 97404 dell'esercizio finanziario 2025;

Il Direttore del Dipartimento
Prof. Stefano Romano

Catania, 21/10/2025

DIPARTIMENTO
FISICA E ASTRONOMIA
"Ettore Majorana"

Prot. 197652 del 21/10/25

INVOICE

Springer Nature Customer Service Center GmbH www.springernature.com
Europaplatz 3
69115 Heidelberg | Germany
VAT ID.DE209719094

SPRINGER NATURE GROUP

Our Reference No.	Finance Account No.	Customer Account No.	Purchase Order No.	Customer VAT ID	Date	Pages
> 2936578900	> 2201313965	> 3007795038	>	> IT02772010878	04.08.2025	1 / 2

Bill to

> University of Catania
Dept. Physics and Astronomy
Via Santa Sofia 64 6
95125 Catania
Italy

Ship to

Salvo Mirabella
University of Catania
Via Santa Sofia 64 6
95125 Catania
Italy

Quantity	Product No.	Description	List Price	Disc. %	VAT	Amount
1	43930E	Single APC Order: 0019701880 Open: Man Apc price Open: man.ReducePr. Open:APC+ Discount	2.390,00 2.390,00		A	2.390,00
		Manuscript ID: 452BB9AC-BF65-480C-A0B4-B3F20E9721E DOI:10.1038/S41598-025-13853-Z Journal Name: Scientific Reports Author Name: Salvo Mirabella Manuscript Title:Molybdenum carbide nanoparticles produced by pulsed laser ablation for efficient hydrogen evolution reaction in alk Customer to self-assess VAT (reverse charge), Article 44 & 196 of EC Directive 2006/112				
1	80078E	Single APC Admin Fee Order: 0019701880 Open: Admin Fee Customer to self-assess VAT (reverse charge), Article 44 & 196 of EC Directive 2006/112	55,00		A	55,00

VAT Reverse Charge, the customer is liable for the VAT due

The European Union's (EU) General Product Safety Regulation (GPSR) is a set of rules that requires consumer products to be safe and our obligations to ensure this.

If you have any concerns about our products, you can contact us at: ProductSafety@springernature.com

In case Publisher is established outside the EU, the EU authorized representative is:
Springer Nature Customer Service Center GmbH
Europaplatz 3
69115 Heidelberg, Germany

FATT. INTRA U.E. n° 7/2025

	Subtotal	2.445,00

INVOICE

Springer Nature Customer Service Center GmbH www.springernature.com
Europaplatz 3
69115 Heidelberg | Germany
VAT ID.DE209719094

SPRINGER NATURE GROUP

Our Reference No.	Finance Account No.	Customer Account No.	Purchase Order No.	Customer VAT ID	Date	Pages
> 2936578900	> 2201313965	> 3007795038	>	> IT02772010878	04.08.2025	2 / 2

Net Value Goods C	0,00	Net Value Goods B	0,00	Net Value Goods A	2.445,00	Total Net Value of Goods	2.445,00
Net Shipping Costs C	0,00	Net Shipping Costs B	0,00	Net Shipping Costs A	0,00	Total Net Shipping Costs	0,00
Total Net C	0,00	Total Net B	0,00	Total Net A	2.445,00	Total Net Due	2.445,00
Incoterms DDP	VAT C	VAT B		VAT A		Total VAT	0,00
						Subtotal	2.445,00
						Prepaid	0,00
						TOTAL DUE EUR	2.445,00

Questions regarding this order?
> Fon: +44(0) 293 192 2009
For queries or assistance, please contact
ORSupport@springernature.com
For Remittance Advice and proof of payment, please email them at **ARadvice@springernature.com**
For overdue and pre collection letters:
Collections.OpenAccess@springernature.com
For supplier Portal and Invoice upload contact
orsupportadmin@springernature.com

Remit a payment in Euro to:
Bank details: **Hypovereinsbank München**
Account: 654793298 - Sort code : 70020270
IBAN: DE22 7002 0270 0654 7932 98
BIC: HYVEDEMMXXX

To pay by credit card:
Scan QR-code or send an E-mail to:
creditcard@springernature.com
for a secure payment link
Do not send us your credit card details

Payable net 30 days

Thank you for your order.

Università degli Studi di Catania

DIP. FISICA ED ASTRONOMIA

C.F. 02772010878

Codice	I_ACQSERVIZI_55
Esercizio	2025
Numero	69
Data	21/10/2025

DA CITARE NELLE FATTURE, NELLE RELATIVE COMUNICAZIONI E SUGLI IMBALLAGGI

Dati per Fattura Elettronica

Codice Univoco Ufficio: UFYX1G
Riferimento Amministrazione: DFA

SPRINGER NATURE CUSTOMER SERVICE CENTER GMBH

Europaplatz 3

99146 69115 HEIDELBERG
P. IVA DE209719094

CUP: Come indicato nei dettagli
CIG B8B53AD753

Descrizione Ordine

Condizioni di pagamento	30 D.Ric.F.
Vs. riferimento	INVOICE 2936578900 DEL 04/08/2025
Descrizione	N.I. 243 - PUBBLICAZ. SCIENTIFICA PROF. MIRABELLA

Descrizione	Q.tà	Prezzo Unitario	Sconto (%)		Importo Imponibile	Importo Iva compresa
PUBBLICAZ. SCIENTIFICA PROF. MIRABELLA Cod. CUP:E53D23016050001. Cod. CIG: B8B53AD753 Causale EP:D20-Servizi per pubblicazioni d'Ateneo	1,00	€ 2.445,00			€ 2.445,00	€ 2.445,00
				Totale	**€ 2.445,00**	**€ 2.445,00**

Es.Mov	N.Mov.	Movimento	Data	Descrizione	Capitolo/UPB	Importo
2025	194406	Impegno di budget	21/10/2025	N.I. 243 - PUBBLICAZ. SCIENTIFICA PROF. MIRABELLA	15088811 Spese per le pubblicazioni scientifiche dell'Ateneo 55723062020	€ 2.445,00
2025	194407	Impegno di budget	21/10/2025	N.I. 243 - PUBBLICAZ. SCIENTIFICA PROF. MIRABELLA	15088811 Spese per le pubblicazioni scientifiche dell'Ateneo 55723062020	€ 537,90
					Totale degli impegni di spesa	**€ 2.982,90**

Note:
CLAUSOLE CONTRATTUALI

Al fine di agevolare il corretto e tempestivo recapito della fattura alla struttura di pertinenza per le operazioni di contabilizzazione e di pagamento, il tracciato della stessa dovrà obbligatoriamente contenere, nei campi appositamente predisposti, i seguenti codici, inclusi quelli non obbligatori:

<Codice Destinatario> Codice Univoco Ufficio <Codice Unitario Progetto> Codice CUP <Codice Identificativo Gara> Codice CIG <altra informazione> Codice riferimento amm.ne <Dati ordine acquisto> Numero buono ordine

- Codice Univoco Amministrazione – UFYX1G
- Codice di riferimento amministrazione - DFA
- Codice CIG, tranne i casi di esclusione dall'obbligo di tracciabilità di cui alla Legge n. 136 del 13 agosto 2010;
- Codice CUP, ove richiesto.

Inoltre, nel campo descrittivo della fattura, dovrà essere riportato il richiedente e il numero di impegno desumibili dal buono d'ordine.

L'inserimento dei predetti codici è condizione indispensabile affinché la fattura possa essere accettata dall'Ente.

Condizioni di pagamento pattuite: 30 gg data ricezione fattura.

Il richiedente dichiara di aver preso visione delle Convenzioni attive sul sito del Ministero dell'Economia e delle Finanze – CONSIP (www.acquistinretepa.it) e dichiara pertanto di: acquistare prodotti non disponibili su convenzioni CONSIP.

Università degli Studi di Catania

DIP. FISICA ED ASTRONOMIA

C.F. 02772010878

Codice	I_ACQSERVIZI_55
Esercizio	2025
Numero	69
Data	21/10/2025

DA CITARE NELLE FATTURE, NELLE RELATIVE COMUNICAZIONI E SUGLI IMBALLAGGI

Per Accettazione
L'operatore Economico

Il Direttore

UNIVERSITÀ degli STUDI di CATANIA

Dipartimento di Fisica e Astronomia "Ettore Majorana"

Catania, 1 | 9 | 2025

Prot. N	0 / 0
Alleg.	
N.rich.	243

a cura dei servizi istituzionali

Id.gest.	cod.contab.	ente

a cura dei servizi finanziari

Al Funzionario responsabile dell'Ufficio Finanziario

e p.c. : Al Dirigente A.FI

Oggetto: nota istruttoria n. 243

Struttura richiedente			
Descrizione		cod.contab.	
C.R.	Dipartimento di Fisica e Astronomia "Ettore Majorana"		(Dipartimento)
C.C.			(struttura interna richiedente)
DOC.	MIRABELLA SALVATORE		(titolare del fondo)
a cura	servizi istituzionali	servizi finanziari	

Spesa finalizzata (1):	
	Forniture
	Utenze
X	Servizi (incluso manut. attrezzature)
	Missioni
	Contratti co.co.co o occasionali
	Contratti d'insegnamento
	Assegni di ricerca
altro:	

Inoltrare le richieste per singola tipologia

La spesa viene imputata :		Finanziam.interno	Finanziam.esterno
	Budget Dipartimento		
	C/ Terzi		
	Fondi di Ricerca		X
	Altri Fondi di Provenienza Esterna		

a cura dei servizi istituzionali

RUP	GIUDICE Nunzio

(1) Specificare in dettaglio la spesa da sostenere per singola tipologia

Interventi	DESCRIZIONE ANALITICA DELLA SPESA	IMPORTO	DESCRIZIONE DEL CAPITOLO	CODICE CAPITOLO	ES.	Impegno provvisorio	Co.An.
1	Pagamento APC pubblicazione scientifica	2.982,90 €	PRIN	15088811	25	97404-2	A20
2	IVA	656,24				97405-2	
3							
4							
5							
6							
7							
8							
	Totale	2.982,90 €					

a cura dei servizi istituzionali — a cura dei servizi contabili

Ulteriori informazioni

DOCUMENTAZIONE ALLEGATA

a cura dei servizi istituzionali

Il Direttore del Dipartimento

Il Responsabile dell'Ufficio Amministrativo e del Personale

Il Responsabile dell'Ufficio Finanziario

N.	Consegnatari	Ubicazioni
*	URSO MARIO	
1	URSO MARIO	DFA - UniCT
2		
3		
4		
5		
6		
7		
8		

* Consegnatario di tutta la N.I.

Direzione amm.va Aree	competenza conoscenza	Uffici Dipartimentali	competenza conoscenza
Direzione amm.va	X		
AFI	X	AMM	X
ARIT		AFI	XX
ACUC		PROV-ECON	XX
ADI		DIDATTICA	
AGAP		RICERCA	
ULA		BIBLIO	
ASI			
ARI			

X = Conoscenza XX = Competenza

compilazione a cura dei servizi istituzionali

trasmissione a cura dei servizi finanziari

Situazione del movimento finanziario di spesa

Ente	
Nome Ente	**Università degli Studi di Catania**
Nome Dipartimento	

Esercizio finanziario 2025

Fase precedente Impegno Provvisorio n.2746/2025

Descrizione: N.I. 243/25 PUBBL. SC. APC

UPB: 55723062020 (PRIN 2022 PNRR Settore PE5 progetto "IMAGE" prof. S. Mirabella)

Bilancio: Articolo 15088811 (Spese per le pubblicazioni scientifiche dell'Ateneo)

CUP: E53D23016050001

1. Importo originale	€	2.982,90
2. Variazioni Esercizi Prec.		
3. Variazioni Esercizio Corr.		
4. Importo comprensivo delle variazioni (1 + 2 + 3)	€	2.982,90
6. Totale movimenti (Impegno di budget) eserc. precedenti		
7. Totale movimenti (Impegno di budget) eserc. corrente		
8. Totale variazioni (Impegno di budget) eserc. precedenti		
9. Totale variazioni (Impegno di budget) eserc. corrente		
10. Importo Disponibile (4 - 6 - 7 - 8 - 9)	€	2.982,90
6. Totale movimenti (Liquidazione) eserc. precedenti		
7. Totale movimenti (Liquidazione) eserc. corrente		
8. Totale variazioni (Liquidazione) eserc. precedenti		
9. Totale variazioni (Liquidazione) eserc. corrente		
10. Importo Disponibile (4 - 6 - 7 - 8 - 9)	€	2.982,90

Situazione al 10/10/25

Prenotazione di budget n° 97404 del 2025 Data contabile 10/10/25

I/B 196406

I/B 196407 IVA

00.AN. D20

Da: **Nunzio Giudice** nunzio.giudice@ct.infn.it
Oggetto: N.I. n. 243/2025 prot. n. del 21/10/2025
Data: 21 ottobre 2025 alle ore 10:46
A: davide.vigneri@unict.it

Con riferimento alla procedura in oggetto si trasmette il CIG B8B53AD753 .
Si propone di procedere con affidamento diretto all'OE 'SPRINGER NATURE GROUP' ai sensi dell'art. 50, co.1 lett. b) del Dlgs n. 36/2023.
Si allegano alla presente:

- VERIFICA PARTITA IVA ESTERA

- CIG

NUNZIO GIUDICE
VICE-Responsabile Ufficio di Coordinamento dei Laboratori DFA ed.6
University of Catania & INFN
Via S. Sofia 64
95123 Catania Italy
Phone +39 095 378 53 49
Mobile +39 393 02 02 319
E-mail: nunzio.giudice@ct.infn.it
at CERN, Geneva (Switzerland)
E-mail: nunzio.giudice@cern.ch

Piattaforma Contratti Pubblici _ Portale Servizi A.N.AC..pdf

Vies on-the-Web - European Commission https://ec.europa.eu/taxation_customs/vies/#/vat-validation-result

Commissione

ITA

AUTORITÀ NAZIONALE ANTICORRUZIONE

Home / Piattaforma Contratti Pubblici / Le Tue Procedure / Gestione Dettaglio Procedura / Dettaglio Lotto

NG Nunzio Giudice
UNIVERSITA' DEGLI STUDI DI CATANIA

MENÙ

- Dashboard
- Le Tue Bozze
- Le Tue Procedure
- Verifiche Preliminari
- Servizi

DETTAGLIO LOTTO

Dettaglio procedura

Dettaglio Lotto

Progressivo lotto
LOT-0001

Stato lotto
Aggiudicato

CIG

B8B53AD753

Fase

Affidamento

Importo Lotto

2445

Oggetto

NOTA ISTRUTTORIA 243 SPRINGER NATURE GROUP

Prosegui Lotto

Azioni eseguite

CONTATTI

protocollo@pec.anticorruzione.it

Contact Center
+39 06 62289571

QUICKLINKS

Portale istituzionale

Portale servizi

Amministrazione trasparente

V. 1.1.1

UNIVERSITÀ degli STUDI di CATANIA

Dipartimento di Fisica e Astronomia "Ettore Majorana"

206/2025

Prot n.
Allegati:

All'ufficio amministrativo e del personale

All'ufficio provveditorale

RICHIESTA AFFIDAMENTO SERVIZIO O FORNITURA

OGGETTO:	[X] SERVIZIO	[ ] FORNITURA
	Pagamento "Article Processing Charge" per pubblicazione scientifica sulla rivista Scientific Reports	
MOTIVAZIONI CHE GIUSTIFICANO LA RICHIESTA		
MOTIVAZIONI CHE GIUSTIFICANO L'EVENTUALE URGENZA		
IMPORTO PRESUNTO (comprensivo di eventuali rinnovi)	[X] sino a € 10.000,00	€ 2.445,00 escluso I.V.A.
	[ ] compreso tra € 10.000,00 e € 40.000,00	€ 0,00 escluso I.V.A.
	[ ] superiore a € 40.000,00	€ 0,00 escluso I.V.A.
Clausole essenziali del servizio/fornitura richiesto		
DATI BILANCIO	IMPORTO PRESUNTO FORNITURA: € 2.982,90 (compreso IVA)	
	Accantonamento Funzioni Tecniche - "Regolamento per la ripartizione dell'incentivo delle funzioni tecniche di cui all'art.45 del D.lgs. 36/2023": € 48,90	
	UPB: DESCRIZIONE: IMAGE	
CUP (ove previsto)		
Subconsegnatario:	URSO MARIO	
Ubicazione:	DFA - UniCT	

Catania, 05/08/2025.

Il richiedente.

URSO MARIO
Firmato il 27/08/2025 (*)

I titolari dei fondi.

MIRABELLA SALVATORE
Firmato il 27/08/2025 (*)

(*)Il documento è firmato con 'firma elettronica avanzata' ai sensi del D. Lgs. 82/2005 s.m.i. e norme collegate e sostituisce il documento cartaceo e la firma autografa.

DETTAGLIO RICHIESTA AFFIDAMENTO SERVIZIO O FORNITURA #206/2025

Descrizione	Subconsegnatario	Ubicazione	Quantità	Prezzo	Sconto%	I.V.A.%	Totale
Pagamento APC pubblicazione scientifica	URSO MARIO	DFA - UniCT	1	2.445,00	0	22	2.982,90

scientific reports

Check for updates

OPEN

Molybdenum carbide nanoparticles produced by pulsed laser ablation for efficient hydrogen evolution reaction in alkaline conditions

Valentina Iacono[1,2], Helena Rabelo[3], Cristiano Lo Po'[1], Luca Pulvirenti[4], Maria Chiara Spadaro[1,2,3], Jordi Arbiol[3,5], Francesco Ruffino[1,2,6] & Salvo Mirabella[1,2]✉

Molybdenum carbides have emerged as an optimal alternative to noble expensive materials for hydrogen evolution reaction (HER). Most reported synthesis methods involve prolonged operations at high temperatures in reactive gases environments. In this study, we introduce nanosecond Pulsed Laser Ablation in Liquid (PLAL) as a viable and environmental friendly approach for synthesizing molybdenum carbide by ablating a molybdenum (Mo) target in ethanol. Structural and compositional characterizations on the nanoparticles (NPs) reveal no oxidation and the absence of a graphitic shell, confirming the formation of hexagonal Mo_2C and cubic MoC. The NPs loaded on nickel foam exhibit significant HER activity in an aqueous 1 M KOH electrolyte, with a potential of 136 mV vs. RHE at 10 mA cm^{-2} and 240 mV at 50 mA cm^{-2}. The calculated mass activity (0.05 A/cm^2) highlights the high intrinsic activity of this material compared to conventional and non-green synthesis methods reported in literature.

Keywords Pulsed laser ablation in liquid, Molybdenum carbide, Nanoparticles, Hydrogen evolution reaction

According to the International Energy Agency (IEA) a global energy crisis is affecting all countries in the energy production market, requiring more and more effort in clean energy source production[1]. Hydrogen is a promising key player, with the highest energy density among energy vectors, still its sustainable production at large scale is hindered by proper catalysts availability. Green hydrogen is produced through electrocatalytic water splitting driven by renewable energy through Oxygen Evolution Reaction (OER) and Hydrogen Evolution Reaction (HER) taking place in an electrochemical cell[2]. Large scale production of H_2 takes place in alkaline-based electrolysers with highly concentrated KOH solution, still the development of electrochemically active catalysts is a current great challenge[3]. Noble and precious metals (such as platinum, palladium, iridium) are the most well performing materials but large-scale applications are limited by their high cost. As an alternative, material scientists have shifted their investigation towards low cost and earth abundant materials, such as transition metal carbides (TMCs) showing stability and insolubility and promising catalytic properties, comparable to those of Pt-group metals[4–7].

Molybdenum-based carbides are ultra-hard, resistant materials with metallic conductivity, mechanical strength, high specific conductance and capacitance[7]. Molybdenum carbide can be synthesized in mainly five crystal structures: α-MoC_{1-x}, α-Mo_2C, β-Mo_2C, γ-MoC and η-MoC. A hexagonal crystal structure is exhibited by γ-MoC and η-MoC. Instead, α-MoC_{1-x} has face centered cubic (fcc) structure. The α-Mo_2C orthorhombic close packed (hpc) structure is due to Mo and C layers placed in alternating order while β-Mo_2C has a hexagonal crystal structure[8,9]. Due to its d-band electronic structure similar to Pt, it is a relevant material as an electrochemical catalyst for HER. The similarity with Pt structure arises from C occupying interstitial spaces within the Mo metal lattice, during the carbide formation, causing the lattice expansion and a consequent shift of the metal d-band and an increase of valence electrons density[10].

[1]Dipartimento di Fisica e Astronomia "Ettore Majorana", Università di Catania, via S. Sofia 64, Catania 95123, Italy. [2]CNR -IMM, Catania Università, via S. Sofia 64, Catania 95123, Italy. [3]Catalan Institute of Nanoscience and Nanotechnology (ICN2), CSIC and BIST, Campus UAB, Bellaterra, Barcelona 08193, Catalonia, Spain. [4]Dipartimento di Scienze Chimiche, Università di Catania, Viale Andrea Doria 6, Catania 95125, Italy. [5]ICREA, Pg. Lluís Companys 23, Barcelona 08010, Catalonia, Spain. [6]Research Unit, University of Catania, National Interuniversity Consortium of Materials Science and Technology (INSTM-UdR of Catania), Viale Andrea Doria 8 and Via S. Sofia 64, Catania 95125, Italy. ✉email: salvo.mirabella@dfa.unict.it

The investigation on this material and its electrochemical properties have shown how this material can have low overpotential for HER, even lower than 0.1 V (vs. RHE) at 10 mA cm^{-2} and 0.3 V at 500 mA cm^{-2}, in acidic and alkaline electrolyte and great stability[10]. The synthesis of this material has been exploited not only as nanostructures but also as homogeneous layer of carbide starting from a Molybdenum substrate, making the material more robust. An example about this last strategy was reported by W. Liu el al. in which a Mo substrate surface was turned into MoC / Mo_2C in molten carbonate where CO_2 was reduced to C allowing a carbide layer formation[11]. This process led to a durable and highly active catalyst for HER, better than Pt. Most of the reported works about Mo_xC, although the outstanding performance reported, use high temperature processes (700–1000 °C), flammable gases use and long-time operation (4–6 h)[12]. Moreover, the produced material often aggregates pouring the accessible active sites for catalytic activity. Hence, the inclusion of other metals (like Nickel) atoms or coating/supporting carbon nanomaterials has been considered to improve water splitting performance[10,13,14].

Pulsed Laser Ablation in Liquid (PLAL) is an optimal and alternative candidate for synthetizing Mo carbide. The out-of-equilibrium condition created by the laser-matter interaction involving a Mo target, a C-based solvent (like acetone or ethanol) results on target vaporization and inclusion of carbon atoms. PLAL implies the use of a high-power pulsed laser focused onto a metallic target leading to localized high temperature (thousands of kelvins) heating and to bubble formation with following reaction among target atoms and solvent molecules[15]. Some advantages of this technique are the synthesis of pure and ligand-free nanoparticles (NPs). The obtained NP dispersion does not need any post-synthesis treatment or washing, reducing the number of preparation steps. Furthermore, its energy consumption is limited without the need for additional temperature and pressure control systems. Due to these advantages, PLAL has recently been exploited for the facile and rapid synthesis of highly active electrocatalytic NPs, with performances superior or comparable to those of NPs synthesized with other techniques[16,17]. To this end, due to the high energy provided by the laser and the interaction among a C-rich solvent and Mo target, PLAL can be considered more environmentally friendly than conventional approaches for the synthesis of transition metal carbides. Although industrial scale-up remains a challenge, the potential of the PLAL approach is increasingly evident[10].

Concerning the synthesis of Mo_xC materials, it is not quietly new for laser ablation techniques. In 2013, L. Franzel et al. reported the synthesis of Mo/MoC nanoparticles (NPs 4 nm medium size) by laser ablation of a Molybdenum target immersed in Ethanol using a picosecond pulsed laser[18]. Femtosecond pulsed laser induced the formation of MoC NPs (60 nm diameter) with graphite shell irradiating a Molybdenum target in Hexane environment[19] .

Nanosecond pulsed laser ablation was exploited in toluene with N_2 atmosphere resulted in MoC NPs while in ethanol have been obtained MoC/ C core shell NPs and small Mo_2C NPs using a lower power ns-laser[20,21]. These examples have shown how the non-equilibrium conditions of laser ablation involving organic solvent as liquid environment led to the inclusion of carbon in the target atoms, making this technique suitable for carbides material synthesis. Short pulse ablation has shown the capability of synthetizing MoC /C NPs. On the other hand, for nanosecond ablations none has reported carbide NPs (MoC and Mo_2C) with the absence of carbon shells and no investigation about the electrochemical properties of these materials for HER was considered.

In this work, we demonstrate the production of Molybdenum Carbide NPs with the use of a nanosecond pulsed laser by the ablation of a Mo target immersed in Ethanol. The material produced as NPs dispersion was characterized in terms of morphology, compositional and structural properties. Then, the NPs were tested as electrocatalysts for HER in alkaline environment showing promising results.

Results

Synthesis and characterization of molybdenum carbide NPs

Figure 1 (a) shows the schematic of PLAL process used for the synthesis of MoC/Mo_2C NPs. The scheme displays the infrared laser beam exiting from the Nd: YAG ns-laser focused onto the metallic target immersed in Ethanol.

Due to the interaction between the laser and the metallic target, a plasma plume is formed during which the metal atoms from the target interact with the solvent molecules, finally producing a NPs dispersion[22]. In this work, 5 min of laser ablation causes 0.4 mg of mass loss of the target. After the synthesis, 10 uL of the NPs dispersion was drop cast onto a Silicon substrate and the SEM analysis was performed. In Fig. 1b, SEM shows how the NPs possess a spherical geometry, a few NPs has a diameter of almost 1 μm, but the majority of them has a size of 20–30 nm. In order to better analyze the size distribution of the NPs (Fig. 1d) HAADF STEM measurements were performed (Fig. 1c). The curve representing the size distribution is a lognormal whose highest peak is centered on 14.5 nm as most representative size of the NPs. This curve well represents the data collected and it is the one expected for NPs obtained by PLAL[23].

STEM-EELS experiment was conducted focusing onto Mo M-edge at 227 eV (green), C K-edge at 284 eV (red), O K-edge at 532 eV (blue) and N K-edge at 401 eV (violet). The outcoming images (Fig. 2a) show that Molybdenum and Carbon coexist within the NPs. Some Oxygen surrounds them within being part of the inner composition, probably because of the oxygen content in the solvent used as ablation environment and air exposure prior to the TEM experiments. The Nitrogen signal is given by the TEM grid support.

With electron microscopy-based methodologies in transmission mode it was possible to evaluate the crystal structure of the synthesized material, via power spectra (FFT) analysis, and elemental distribution, via STEM-EELS maps. HRTEM images and corresponding power spectra (Fig. 2b) showed that the NPs possess a good crystal structure and some defects, like twin boundaries as evidenced in Figure S1. The FTT patterns derived agreed with the cubic Fm3m phase MoC and, some NPs also, agreed with the orthorhombic Pbcn phase of Mo_2C.

More about the structural properties of the NPs was investigated with XRD measurements. The XRD pattern in Fig. 2c shows the peaks related to the MoC cubic structure (corresponding to the space group Fm-3 m (225)

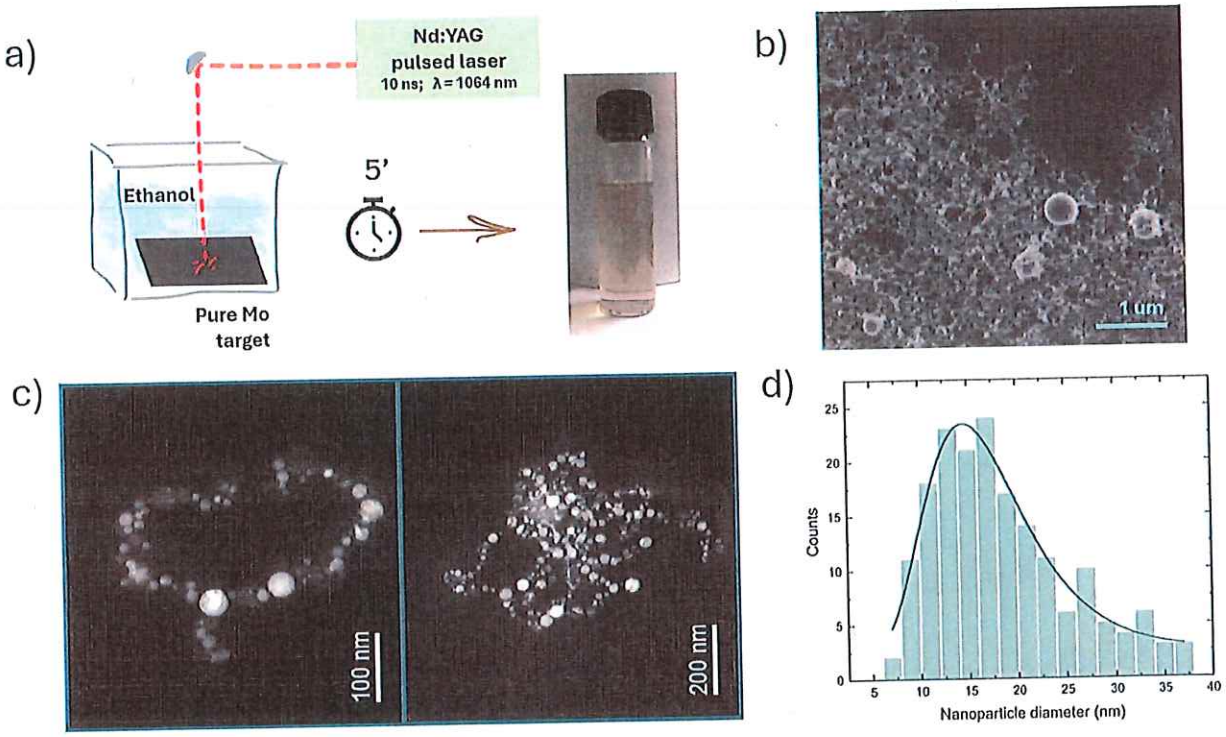

Fig. 1. (a) Schematic of PLAL system in which the Nd: YAG pulsed laser is focused onto the Mo target immersed in Ethanol. After 5 min of ablation, 8 mL of NPs dispersion into the vial appear brown/grey. (b) Low magnification SEM of NPs onto Si substrate. (c) Low magnification HAADF STEM images of NPs. (d) NPs size distribution derived from the HAADF STEM images. The curve fitting the data follows a lognormal distribution whose maximum value is centered at 14.5 nm.

(PDF Card No.: 00-065-0280) and also the peaks referred to hexagonal Mo_2C (PDF Card No.: 00-011-0680) related to the space group: P63/mmc(194)[24]. These characterizations showed that there is no evidence of the MoO_3 presence in the NPs that consist of cubic MoC or hexagonal Mo_2C crystals.

The surface chemical composition of the obtained NPs was then investigated by X-Ray Photoelectron Spectroscopy. As Figure S3a shows, the Mo 3d region was deconvoluted in four components. Peaks at 227.3 eV and 228.5 eV were assigned to Mo carbides (MoC or Mo_2C) and metallic Mo^0, respectively. Contributions at 231.1 eV and 232.5 eV correspond to Mo^{4+} and Mo^{6+} oxidation states, and are ascribed to oxidized molybdenum species likely formed upon air exposure of the NPs surface[11]. The just discussed characterizations show the successful formation of carbide material by laser ablation. The solvent and the target material play a crucial role in carbonization by ablation technique. The carbonization of the metal starts in the plasma phase in which the organic solvent starts to be decomposed under the laser irradiation. The decomposition of organic molecules can generate gases, such as the reductive CH_4 or CO, thus carbon atoms are available for carbonization[21,24,25]. Not all the metals are able to include carbon atoms and for stable carbides. For metals like Cu or Ni, the carbon-metal phase diagram reports that with the temperature decrease, carbon can go toward the formation of a shell instead of forming metal carbide. However, this is not always verified and can strictly depend on the solvent used and the laser synthesis parameters. Those metals with more d-vacancies, like the metals of the IVB- VIIB group, as Mo and W, have a high carbon solubility (~39%) such that the carbon atoms bind at the metals' vacancies[26]. This happens in the gas phase (thus, cavitation bubble) where the temperature is in the proper range (150–490 °C). H. Zhang et al. reported the synthesis of MoC/C core shell NSs by PLAL in Ethanol specifying that the level of the liquid above the target surface is about 10 mm. They observed that larger NSs are MoC/C core/shell NSs and the smaller NPs are orthorhombic Mo_2C[20]. In this work, the presence of carbon or graphitic shell can be excluded by analyzing the HRTEM measurements. This may be an effect due to the liquid height above the target surface (in this case 20 mm) that may have attenuated the laser energy, thus reduced the pyrolysis of the solvent and avoided the carbon graphitization or onion -like organization around the obtained NPs, compared to the other reported PLAL-obtained MoC[26].

In order to sheld light onto Mo-C bonds we employed Raman spectroscopy (Fig. 3a). The most intense peaks observed are at ~661 cm^{-1}, 820 cm^{-1}, and 994 cm are typically related to the Mo_2C phase[27–29]. That small left asymmetry in the 820 cm^{-1} peak, can be associated to the presence of a peak at 805.3 cm^{-1} related to MoC phase. The Raman spectrum also presents the peaks at 1325 cm^{-1} and 1584 cm^{-1} corresponding to the D and G bands of carbon. In particular, the D band is the one associated to disordered carbon framework and the G band indicates amorphous carbon. Some of the peaks in the regions of 100–400 are associated to optical modes

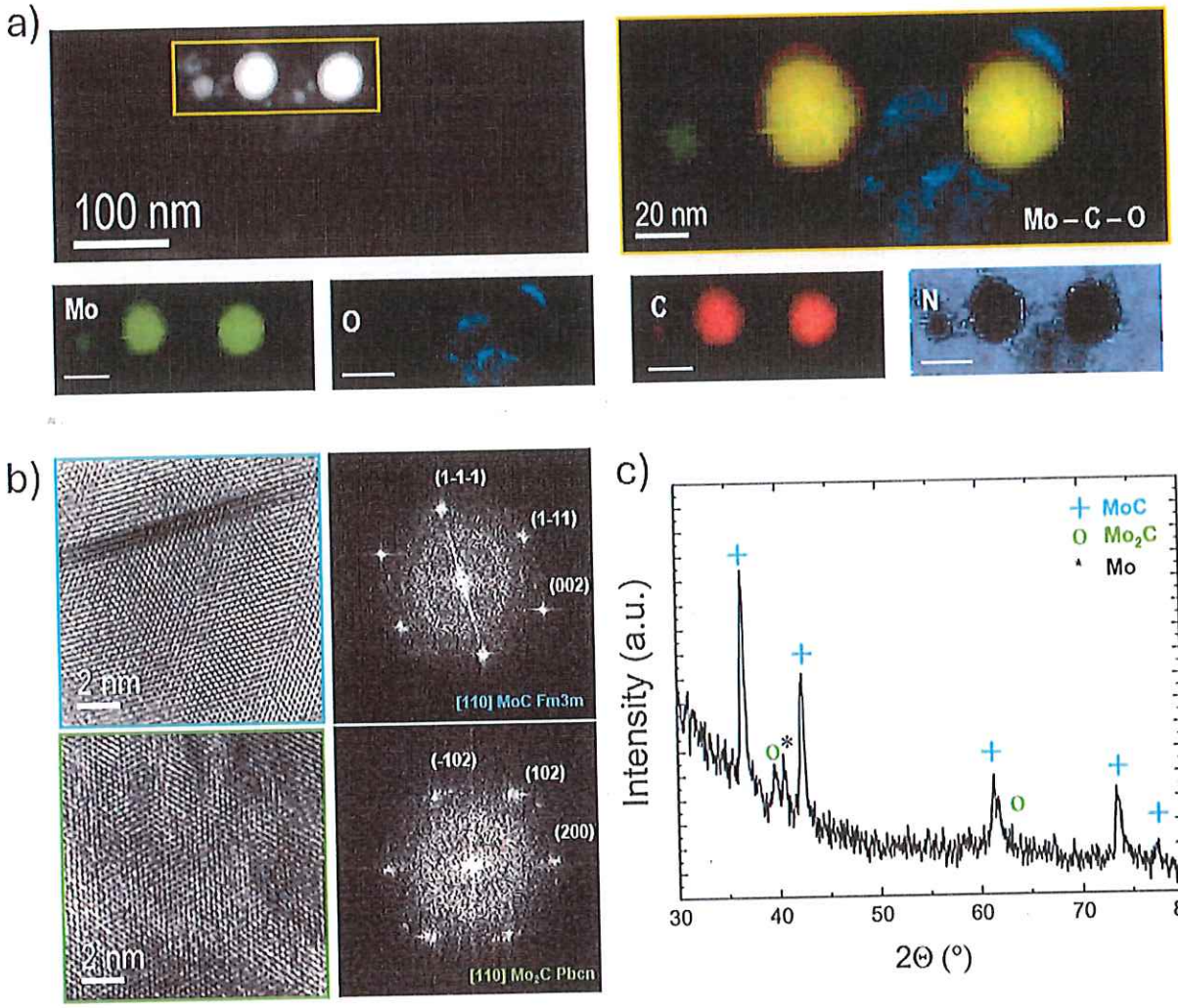

Fig. 2. (a) STEM-EELS maps, focusing on Mo M-edge at 227 eV (green), C K-edge at 284 eV (red), O K-edge at 532 eV (blue) and N K-edge at 401 eV (violet). (b) HRTEM analysis performed for two different NPs with the corresponding power spectrum (FFT) showing both MoC and Mo_2C phases. (c) XRD pattern of the PLAL-obtained NPs with highlighted the Mo, MoC and Mo_2C relative peaks.

of Mo_2C, like 147, 167, 198, 222, 315 cm^{-1}. Also, Tiwari et al., assess the Raman peaks at 280 cm^{-1} and 335 cm^{-1} to E_2g and A_1g vibration modes of Mo_2C[30].

Transmittance measurements were performed onto the NPs loaded onto a fused quartz substrate. Figure S2 reports the transmission spectra obtained for the bare quartz substrate and the NPs loaded one, showing a significant but continuous decrease in transmittance over the entire wavelength range investigated, due to scattering and reflection due to NPs.

No clear evidence of a light absorption gap is given, supporting the hypothesis that the optical bandgap of these NPs should be lower than 0.5 eV, if any. This can be a result confirming the zero optical energy bang gap reported as feature of this material in literature[24,31].

KP AFM measurements were done to exploit the surface properties of NPs. Figure 3b reports three different tip voltage profiles extracted from three line scans of an agglomerated area of NPs (inset, the color scale is related to the height information, the dashed white lines represent the line profile for tip voltage scan). The correspondence with the NPs appears in the increase of the tip voltage signal with respect to the substrate signal (left part of the curves, at ~ -0.280 mV). As the substrate is Au film, whose WF (work function) is reported 5.1 eV, we can assume that the NPs have an average WF of 5.25 eV, compatible with that reported in literature for the β- Mo_2C (001) – Mo exposed phase[31].

These data evidence the successful synthesis of well-defined MoC/Mo_2C nanosized particles by using nanosecond pulsed laser ablation in Ethanol. The presence of Mo_2C, and the absence of a carbon shell, is considered particularly desirable due to Mo_2C superior catalytic activity for HER, as it exhibits stronger proton (H*) adsorption compared to MoC. Given the relatively mild and time-efficient nature of pulsed laser ablation

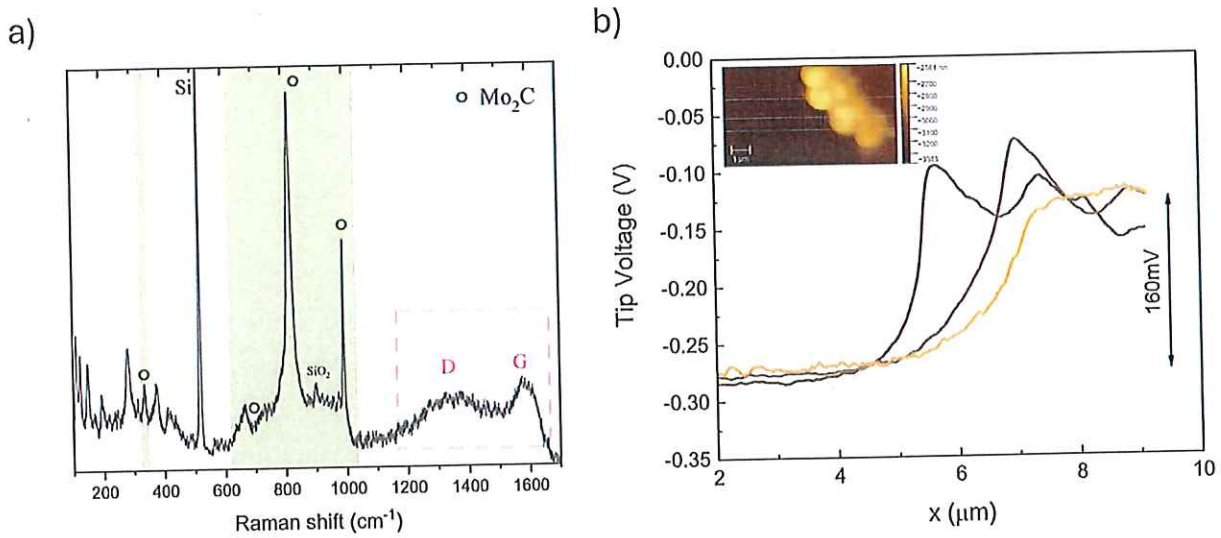

Fig. 3. (a) Raman spectrum of the MoC/Mo_2C NPs. (b) Tip Voltage profiles extracted from KP-AFM. Dashed lines in the inset are the three tip profiles onto the relative topographic image.

in liquid (PLAL) synthesis, especially when compared to the more complex methods reported for this material synthesis, the use of PLAL-synthesized MoC/Mo_2C NPs for alkaline HER is noteworthy.

Investigation on HER mechanism and electrode/electrolyte interface

To study the performance of HER in alkaline aqueous electrolyte, the MoC/ Mo_2C NPs were loaded onto NF to perform electrochemical measurements. SEM image on NPs distributed in the NF substrate is reported in Figure S4a, showing not a full coverage of the substrate. In Fig. 4a, the LSV curves of the bare substrate and the NF+NPs are reported. The loading of 0.2 mg of catalyst (dashed line) is reflected by a significant decrease in the potential vs. RHE @ 10 mA cm^{-2} (from – 0.200 V to -0.135 V vs. RHE). The value of loading was chosen as the optimum, after testing also lower amount of catalyst and different substrate (Figure S5). The significant activity of the PLAL-obtained NPs is also reflected at higher current density (50 mA cm^{-2}) with an overpotential of 239 mV vs. RHE.

After, the LSV measurements, the durability of catalyst activity was then studied by chronopotentiometry measurements in 1 M KOH applying 10 mA/cm^2 for 14 h. The result (showed in Figure S7) reflects a good stability of the electrode over the testing hours. Moreover, SEM image on the used electrode displays the NPs presence on the NF, reflecting not a significant loss of electrocatalyst material (Figure S4b). After HER, the surface composition of the NPs onto the used NF electrode was investigated. The XPS spectrum, showed in Figure S3b, reveals the absence of metallic Mo and still the presence of Mo-carbide peaks, although the percentage of oxide increased, compared to the fresh sample. If considered the exposure to aqueous potassium hydroxide electrolyte, the enhancement of the oxidic species on the surface of the NPs is actually expected.[11].

In Table 1 some Mo_xC carbides are compared in terms of overpotential and mass activity. The comparison reflects how PLAL can be a competitive synthesis approach to get HER-active material without the inclusion of other elements or carbon support. Also, less loading (0.2 mg) is already providing a significant, event lower, activity.

In order to better investigate the HER mechanism catalysed by our NPs, the Tafel plot (Fig. 4b) is now discussed. In alkaline environment, the HER involves the reduction of water molecule toward the production of adsorbed hydrogen atoms on the empty material surface site (*) and hydroxide ions (OH^-)[38,39]. The steps, expressed in reaction as follows, are represented in Fig. 4b bottom. The first step is the Volmer step:

$$H_2O + e^- + * \leftrightarrows *\cdot H_{ads} + OH^- \quad (1)$$

After the Volmer step, Heyrovsky or Tafel step follow:

$$*\cdot H_{ads} + H_2O + e^- \leftrightarrows H_2 + OH^- + * \quad (2)$$

$$2 *\cdot H_{ads} \leftrightarrows H_2 \quad (3)$$

From the Tafel plot (derived from LSV) analysis some hint on the rate determining step (RDS) can be discussed. In our case, the Tafel slope (150 mV /dec) is larger than 120 mV/dec, suggesting that the Volmer step is the one determining the overall rate[38]. In a microkinetical scheme, the electrochemical reactions before the RDS are in quasi equilibrium with the reactants[40,41]. The linear region of the Tafel plot is, indeed, linked to the RDS

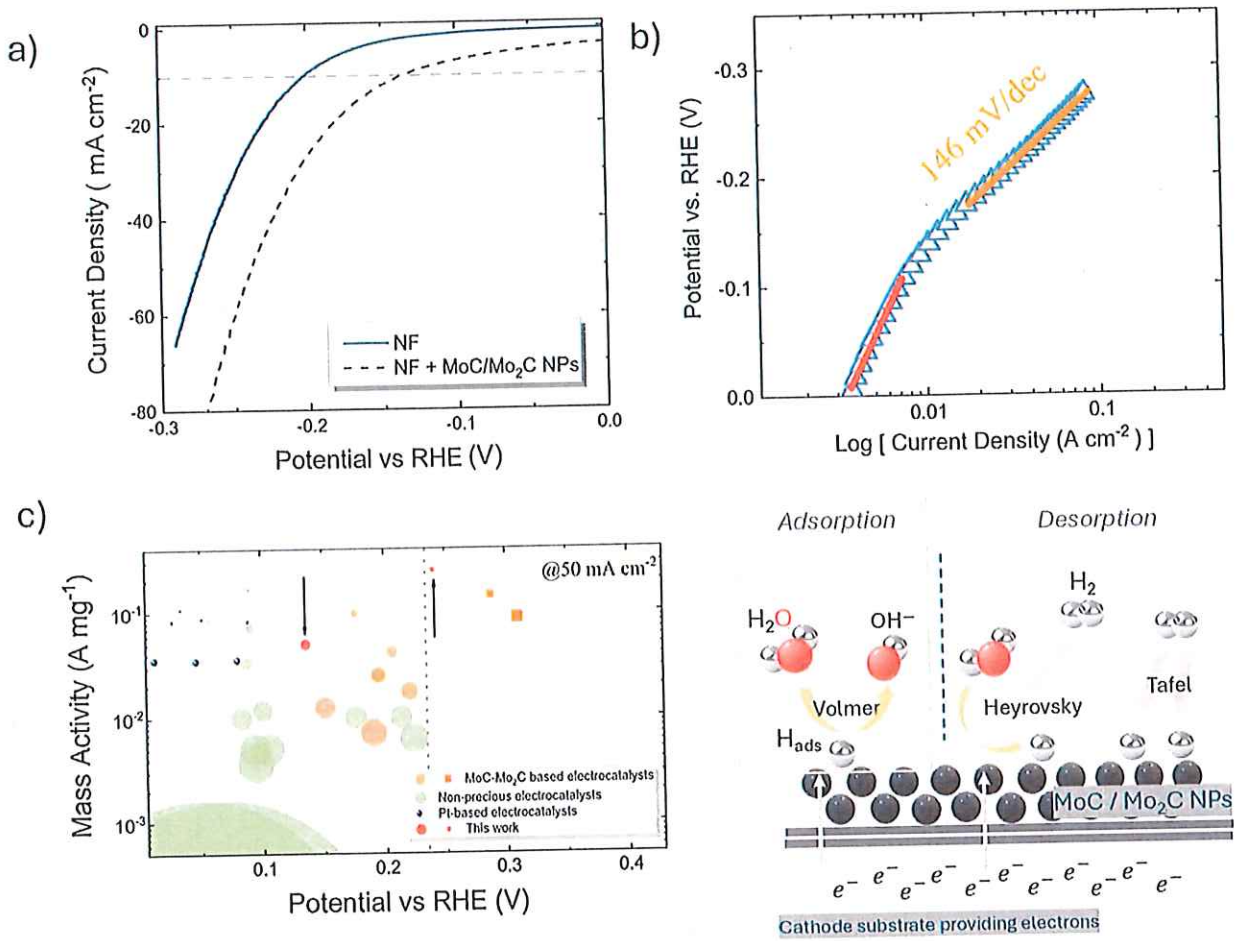

Fig. 4. (a) LSV curve of bare NF and NF with MoC/Mo_2C NPs. (b) Tafel plot of the NF with MoC/Mo_2C NPs electrode with the extracted Tafel slope and, below, the scheme of HER reaction steps in alkaline electrolyte. (c) Mass Activity bubble plot vs. Potential reported at 10 mA cm^{-2} (left) and 50 mA cm^{-2} (right yellowish) for different electrocatalysts in 1 M KOH (data from Table 1 and Ref. [42]).

Catalyst material	Catalyst mass [mg]	Overpotential vs. RHE @ 10 mA cm^{-2} [mV]	Overpotential vs. RHE @ 50 mA cm^{-2} [mV]	Mass Activity @10 mA cm^{-2} [A / mg]	References
Zr-based MOF – MO_2C / NF	1.5-2	174	-	0.005	32
Mo_2C@C	0.24	206	-	0.04	33
β Mo_2C	0.4	195	300	0.02	34
2D MoC /NF	0.4	195	320	0.02	35
MoC/C GCE	0.57	220	280	0.02	36
MoC_x nano-octahedrons	0.8	151	220	0.01	37
MoC/Mo_2C NPs/ NF	0.2	136	239	0.05	This Work

Table 1. Literature comparison among MoC – Mo_2C electrocatalysts reporting the catalyst mass, the overpotential vs. RHE at 10 and 50 ma cm^{-2} and mass activity at 10 ma cm^{-2}.

mechanism[40]. In the Tafel regime, defined as linear region where the overpotential is higher than 30 mV, the Tafel slope (b) can be related as follows:

$$b = \frac{d\eta}{d\log(j)} = \frac{59\frac{mV}{dec}}{\gamma + r_{rds}\,\alpha_{rds}} \tag{4}$$

In which, γ is the number of electrons transferred before the RDS, r_{rds} is assumed 1 (0) when the reaction step has an electrochemical (chemical) nature and is α_{rds} the RDS transfer coefficient, typically in the 0.3–0.7

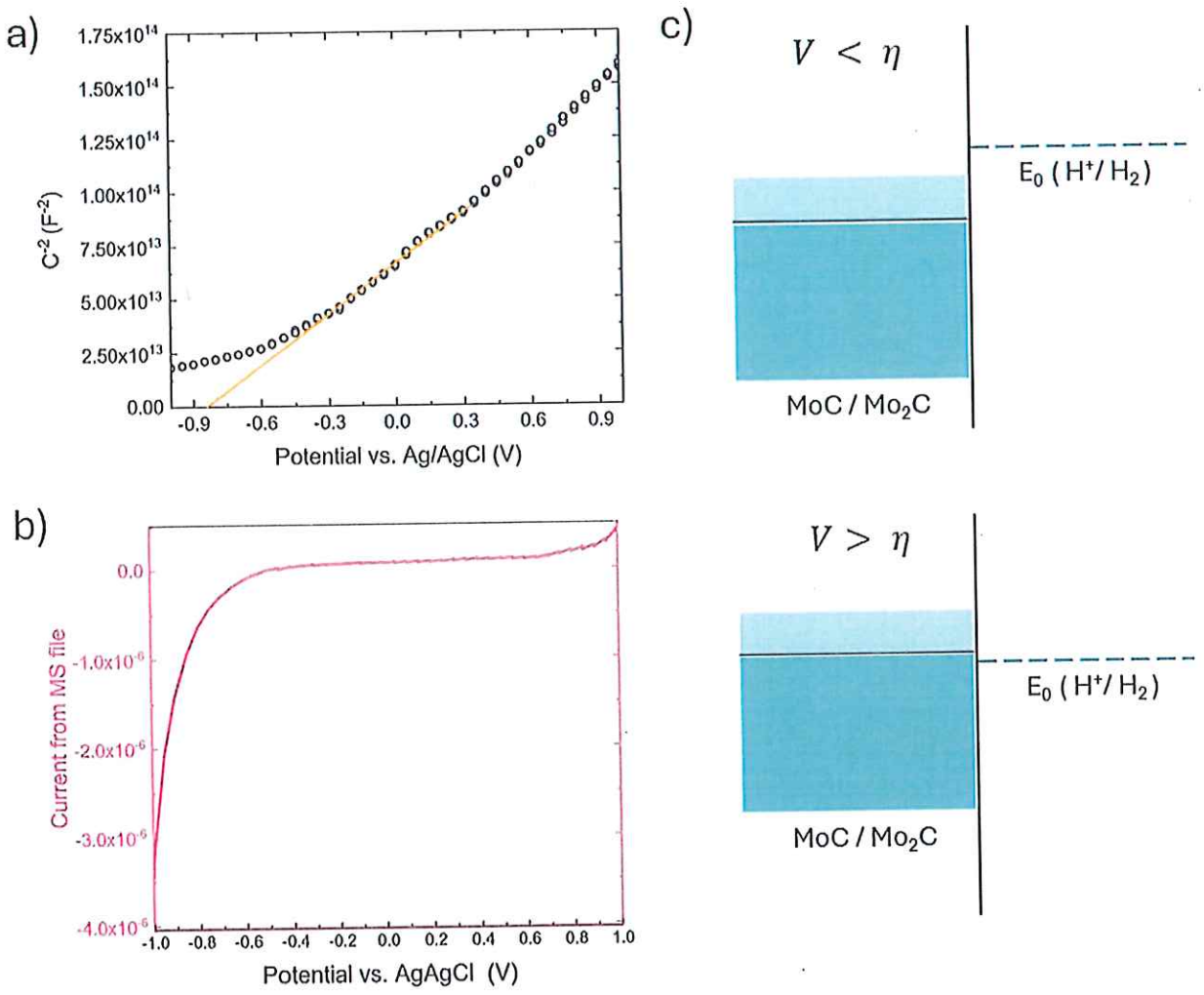

Fig. 5. (a) Mott Schottky and (b) current extracted by the MS measurements for MoC/Mo_2C NPs onto ITO PET in aqueous1 M KOH. (c) Electronic states of MoC/Mo_2C NPs level (to the right) depending on the potential applied (V) respect to the standard potential of hydrogen evolution reaction in the case of V lower (top) of the overpotential and higher (bottom).

range[41]. The value found by analyzing the Tafel plot agrees with $r_{rds} = 1$ and $\gamma = 0$, confirming again the Volmer step as RDS.

In order to evaluate the effective catalyst activity of our PLAL produced NPs, the mass activity (MA) at 10 mA cm^{-2} was calculated to be 0.05 A mg^{-1}.

This result is quite relevant in the literature scenario, in fact, Fig. 4c reports a bubble plot in which MA is reported versus the relative potential for several electrocatalysts at 10 mA cm^{-2} in 1 M KOH (left side, white background)[32–37,42]. The area of each circle represents the catalyst loading. Green circles report some non-precious catalysts (such as Nickel or Cobalt), the dark blue circles are Platinum based electrocatalysts, the orange circles have been added as Mo-based electrocatalysts, and the red circle is related to this work. Platinum based electrocatalysts are well-established top electrocatalysts for HER, even with low catalyst loading Pt points to the top left corner of the plot (the most desirable one). Non-precious catalysts, more abundant and cheaper than Pt, typically stay well below Pt and in particular Mo-based ones show quite large overpotentials for at 10 mA cm^{-2}. Our PLAL synthesized MoC NPs show a promising performance in MA, standing out with respect other Mo-based and non-precious electrocatalysts. The right side of the plot (Havana background) reports some MA data (orange squares) of Mo-based electrocatalysts at 50 mA cm^{-2} compared with our datum (red square). Also at high current, our PLAL synthesized MoC NPs shows results significantly better than those of literature Mo-based electrocatalysts.

Mott-Schottky (MS) analysis was performed to investigate the surface electrode/electrolyte capacitance in the same electrolyte of HER tests. Figure 5a reports MS plot of the NPs sample, while Fig. 5b shows the current measured at the same time from the equipment. MS plot reveals a capacitance increase when negative potentials (vs. RE) are approached.

Such a trend is compatible with a larger availability of charges at electrode surface, sustaining a greater capacitance of the double layer involved (no current is essentially measured for potential down to -0.4 V). The capacitance tends to stabilize when −1 V vs. RE, where a huge current flows because of HER. To interpret this data, the capacitance of the interfacial double layer, $C_{interface}$, should be modelled as the capacitance offered by NPs in series with that of Helmholtz layer[43]:

$$\frac{1}{C_{interface}} = \frac{1}{C_{NPs}} + \frac{1}{C_H} \tag{5}$$

In the case of a semiconductor, the first term is actually the one predominant due to the high density of state of the semiconductor[43]. Whereas in the case of a semimetal (as MoC should be considered), the Helmholtz contribution will be the predominant term[44]. Hence, in the case of a semimetal we cannot mention any band bending at the interface electrode/electrolyte, but we can do a consideration about density of free charge. At the equilibrium (V = 0 V vs. Open Circuit Potential (OCP)) we can think about a low density of free charge due to the presence of electrons-surface states bonding. The electrode/electrolyte area can be imagined as a capacitor with low capacitance. Same, for a potential applied lower than the overpotential. Figure 5c (top) schematizes the free charges level being lower than the energy level for the hydrogen production. Once a more negative potential start to be applied, the capacitance increases as the charge available at the surface increases (like a bigger capacitor with a bigger area) as in bottom part of Fig. 5c, where the applied potential draw the Fermi energy of the electrode higher than that of HER level. The charge becoming more and more available represents the availability of electrons that, at that negative potential, can allow the current increase and, thus, the HER to start.

Summary

In this research study, nanosecond PLAL was employed to synthesize molybdenum carbide by ablating a molybdenum target in ethanol. Morphological and structural analyses revealed spherical nanoparticles (14 nm mean diameter) of cubic MoC and hexagonal Mo_2C structures, with surfaces free of oxidation and graphitic shells. Optical characterization indicated the semimetallic nature of the material, exhibiting a *quasi*-zero bang gap. The NPs, when loaded onto NF, enhanced HER activity, reducing the overpotential to 136 mV vs. RHE at 10 mA cm^{-2} and 239 mV vs. RHE at 50 mA cm^{-2}, using only 0.2 mg of catalyst. Tafel plot analysis identified the Volmer step as the RDS for HER activity. The intrinsic activity, as reflected by the mass activity value, demonstrated competitive performance compared to general transition metal oxide and Mo_xC based nanocatalysts in alkaline electrolyte. In conclusion, ns-PLAL presents a viable alternative synthesis route for producing HER-active molybdenum carbide.

Methods

Synthesis of the molybdenum carbide nanoparticles

A Nd: YAG laser (Quanta-ray PRO-Series pulsed 12 ns) operating at wavelength of 1064 nm, power 5 W and frequency 10 Hz was used for the synthesis of Molybdenum Carbide NPs. The high-power laser beam was focused through a convex lens (focal length 10 cm) on a commercial Molybdenum target (1.5 × 1.5 cm, thickness 1 mm, purity 99.9%) placed at the bottom of a Teflon cylindrical vessel (2.5 cm in diameter), filled with 8 mL of reducing solvent (Ethanol, purity 99.9%) (height liquid above target ~ 20 mm). The estimated fluence value ~ 10 J/cm^2.

After 5 min of ablation, the vessel content became grey colored suggesting the formation of a dispersion of Molybdenum Carbide NPs. The obtained NPs dispersion was stored at 4 °C preserving the stability of the as-synthetized NPs dispersion.

The Mo target was weighed before and after the ablation in order to measure the amount of ablated material from the Mo target. For this measurement a micro analytical balance (Sartorius M5) with a sensitivity of 100 µg was used.

Structural and compositional characterization of molybdenum carbide NPs

Surface morphology of NPs was analyzed by using a Scanning Electron Microscopy (SEM) (Gemini field emission SEM Carl Zeiss SUPRA 25, FEG-SEM, Carl Zeiss Microscopy GmbH, Jena, Germany) using a Silicon substrate with a low amount of NPs drop cast. The same sample was used for recording the Raman spectra using a Horiba Scientific instruments model 1024 × 256-OE, with a laser by THORLABS model HNL225R with a wavelength of 633 nm.

The NPs drop cast onto a fused silica quartz substrate were optically analyzed using a Varian Cary 500 double-beam scanning UV–vis–NIR spectrophotometer measuring the transmittance from 200 to 2500 nm.

The structural properties of the NPs were analyzed through X-Ray diffraction (XRD) measurements. The NPs dispersion was drop cast on a Corning Glass substrate and XRD was carried out in grazing incidence mode (θ_{inc} = 0.5Å°) using a Smartlab Rigaku diffractometer, equipped with a rotating anode of Cu Kα radiation (λ = 1.54056 Å) operating at 45 kV and 200 mA.

The structural analyses have been also performed via High Resolution transmission electron microscopy (HRTEM) in a Tecnai F20 microscope operated at 200 kV. HRTEM was complemented with high-angle annular dark-field (HAADF) STEM images and electron energy loss spectroscopy (STEM-EELS) analyses to evaluate the elemental distribution. By using HAADF STEM images we could extrapolate the diameters of 180 nanoparticles using a Digital Micrograph script in order to obtained the statistical size distribution.

Kelvin Probe Force Microscopy (KPFM) analysis was used to highlight the particle work function. The NPs were drop cast on a silicon substrate previously sputtered with 60 nm of gold. The measurement was conducted

with a Nanosurf DriveAFM in non-contact (called also tapping or dynamic) mode using SCM-PIT-V2 (Bruker) tips with an oscillating frequency of ~75 kHz. An oscillating potential was applied by the machine between the tip and the sample with an amplitude between 2 V and 3 V at a frequency of 20 kHz. The surface potential map was acquired through the second lock-in amplifier of the DriveAFM with a bandwidth of 6 kHz. The measured surface potential is given by the difference between the tip and the sample work function, so the gold film on the substrate was used as reference potential and, in addition, guarantee electrical conductivity[45].

Surface chemical composition of NPs was analyzed by using X-ray Photoelectron Spectroscopy (XPS) (PHI 5000 VersaProbe) with a monochromatic Al Kα source (1486.6 eV) excited by a micro-focused electron beam. Measurements were carried out at a photoelectron take-off angle of 45° relative to the sample surface. The binding energy scale was calibrated using the C 1s peak of adventitious carbon at 285.0 eV.

Electrochemical analysis

The electrochemical measurements performed in this work were done using a Versastat-4 potentiostat and in a three-electrode electrochemical cell using a Pt wire as counter electrode and a Ag/AgCl 3 M KCl as reference electrode. The electrolyte used was 40 mL aqueous solution of 1 M KOH (pH 14).

The electrochemical performance for HER of NPs were studied by using a Nickel Foam (NF) substrate (Goodfellow Inc., Huntingdon, England; thickness 1.6 mm and porosity 95%) loaded with 0.2 mg of NPs after having rinsed with Ethanol and dried in N_2 the substrate. The HER activity of the electrode was investigated using linear sweep voltammetry (LSV) at scan rate of 5 mV s^{-1} in the potential range of 0 - −1.5 V vs. RE. Electrochemical impedance spectroscopy (EIS) was performed with a superimposed 10 mV sinusoidal voltage in the frequency range $10^4 \div 10^{-1}$ Hz at -1.2 V vs. RE. The extracted uncompensated resistance (R_u) was used to determine the iR drop (Figure S6)[46]. The value of the overpotential was taken at a current density of 10 mA cm^{-2} and of 50 mA cm^{-2}. The Mass Activity (M.A.) was evaluated by the ratio between the current density [10 mA cm^{-2}] and catalyst loaded [mg] on the substrate was evaluated in order to compare the intrinsic activity of the electrocatalyst synthesized.

Finally, Mott Schottky analysis was done to extract the capacitance versus the potential. The NPs were loaded onto ITO-PET substrate (ITO film with surface resistivity of 60 Ω/sq from Sigma Aldrich). A small (~2 mm^2) and highly concentrated area was covered with the NPs and properly isolated with a nail lacquer. The amount of NPs on ITO PET was deposited in order to have a sufficiently covered area and isolated in order to avoid substrate contribution. The Mott Schottky measurement was run from −1 to +1 V vs. reference electrode (RE) with a frequency of 1 kHz and an amplitude of 10 mV.

Data availability

The data that supports the findings of this study are available within the article and its supplementary material.

Received: 10 April 2025; Accepted: 28 July 2025
Published online: 04 August 2025

References

1. International Energy Agency World energy outlook 2022. *OECD* https://doi.org/10.1787/3a469970-en (2022).
2. Yao, D. et al. A strategy for Preparing high-efficiency and economical catalytic electrodes toward overall water splitting. *Nanoscale* 13, 10624–10648 (2021).
3. Shiva Kumar, S. & Lim, H. An overview of water electrolysis technologies for green hydrogen production. *Energy Rep.* 8, 13793–13813 (2022).
4. Michalsky, R., Zhang, Y. J. & Peterson, A. A. Trends in the hydrogen evolution activity of metal carbide catalysts. *ACS Catal.* 4, 1274–1278 (2014).
5. Harnisch, F., Sievers, G. & Schröder, U. Tungsten carbide as electrocatalyst for the hydrogen evolution reaction in pH neutral electrolyte solutions. *Appl. Catal. B.* 89, 455–458 (2009).
6. Sokolsky, D. V., Palanker, V. S. & Baybatyrov, E. N. Electrochemical hydrogen reactions on tungsten carbide. *Electrochim. Acta.* 20, 71–77 (1975).
7. Vrubel, H. & Hu, X. Molybdenum boride and carbide catalyze hydrogen evolution in both acidic and basic solutions. *Angew Chem. Int. Ed.* 51, 12703–12706 (2012).
8. Wan, C., Regmi, Y. N. & Leonard, B. M. Multiple phases of molybdenum carbide as electrocatalysts for the hydrogen evolution reaction. *Angew Chem.* 126, 6525–6528 (2014).
9. Guo, J. et al. Insight into point defects and complex defects in β-Mo2C and carbide evolution from first principles. *Materials (Basel)* 15, 4719 (2022).
10. Bae, S. Y., Jeon, I. Y., Mahmood, J. & Baek, J. B. Molybdenum-Based carbon hybrid materials to enhance the hydrogen evolution reaction. *Chem. Eur. J.* 24, 18158–18179 (2018).
11. Liu, W. et al. A durable and pH-universal self-standing MoC-Mo2C heterojunction electrode for efficient hydrogen evolution reaction. *Nat. Commun.* 12, 6776 (2021).
12. Zhou, Z. et al. Recent progress on molybdenum Carbide-Based catalysts for hydrogen evolution: A review. *Sustainability* 15, 14556 (2023).
13. Liu, C. et al. Integration of Ni doping and a mo2c/moc heterojunction for hydrogen evolution in acidic and alkaline conditions. *ACS Appl. Mater. Interfaces.* 13, 22646–22654 (2021).
14. Jia, J. et al. Ultrathin N-Doped Mo2C nanosheets with exposed active sites as efficient electrocatalyst for hydrogen evolution reactions. *ACS Nano.* 11, 12509–12518 (2017).
15. Amendola, V. & Meneghetti, M. What controls the composition and the structure of nanomaterials generated by laser ablation in liquid solution? *Phys. Chem. Chem. Phys.* 15, 3027–3046 (2013).
16. Blakemore, J. D., Gray, H. B., Winkler, J. R. & Müller, A. M. Co_3O_4 nanoparticle Water-Oxidation catalysts made by Pulsed-Laser ablation in liquids. *ACS Catal.* 3, 2497–2500 (2013).
17. Zhou, Y., Dong, C. K., Han, L., Yang, J. & Du, X. W. Top-Down Preparation of active Cobalt oxide catalyst. *ACS Catal.* 6, 6699–6703 (2016).
18. Franzel, L., Phumisithikul, K., Bertino, M. F. & Carpenter, E. E. Synthesis of multiphasic inhomogeneous mo/moc nanoparticles by pulsed laser ablation. *J. Nanopart. Res.* 15, 2032 (2013).

19. Tanaka, Y. et al. Carbonization of a molybdenum substrate surface and nanoparticles by a One-Step method of femtosecond laser ablation in a hexane solution. *ACS Omega.* 8, 7932–7939 (2023).
20. Madrigal-Camacho, M., Vilchis-Nestor, A. R., Camacho-López, M. & Camacho-López, M. A. Synthesis of moc@graphite NPs by short and ultra-short pulses laser ablation in toluene under N 2 atmosphere. *Diam. Relat. Mater.* 82, 63–69 (2018).
21. Zhang, H. et al. A general strategy toward transition metal carbide/carbon core/shell nanospheres and their application for supercapacitor electrode. *Carbon N Y.* 100, 590–599 (2016).
22. Zhang, D., Gökce, B. & Barcikowski, S. Laser synthesis and processing of colloids: fundamentals and applications. *Chem. Rev.* 117, 3990–4103 (2017).
23. Barcikowski, S. et al. Handbook of Laser Synthesis & Processing of Colloids. *DuEPublico: Duisburg-Essen Publications online, University of Duisburg-Essen, Germany* (2019). https://doi.org/10.17185/duepublico/70584
24. Miao, M. et al. Molybdenum Carbide-Based electrocatalysts for hydrogen evolution reaction. *Chem. Eur. J.* 23, 10947–10961 (2017).
25. Saxena, S., Kiefer, J. H. & Klippenstein, S. J. A shock-tube and theory study of the dissociation of acetone and subsequent recombination of methyl radicals. *Proc. Combust. Inst.* 32, 123–130 (2009).
26. Zhang, D. et al. Carbon-Encapsulated metal/metal carbide/metal oxide Core–Shell nanostructures generated by laser ablation of metals in organic solvents. *ACS Appl. Nano Mater.* 2, 28–39 (2019).
27. Upadhyay, S. & Pandey, O. P. One-pot synthesis of pure phase molybdenum carbide (Mo2C and MoC) nanoparticles for hydrogen evolution reaction. *Int. J. Hydrogen Energy.* 45, 27114–27128 (2020).
28. Yuan, M. et al. Atomic and electronic reconstruction in defective 0D molybdenum carbide heterostructure for regulating lower-frequency microwaves. *Adv Funct. Mater* 33, 2302003 (2023).
29. Goyal, R. et al. Synthesis of AgWCNx nanocomposites for the One-Step conversion of cyclohexene to adipic acid and its mechanistic studies. *Chem. Eur. J.* 23, 16555–16565 (2017).
30. Tiwari, A. P. et al. Lattice strain formation through Spin-Coupled shells of MoS_2 on Mo_2 C for bifunctional oxygen reduction and oxygen evolution reaction electrocatalysts. *Adv Mater. Interfaces* 6, 1900948 (2019).
31. Politi, J. R. S., Viñes, F., Rodriguez, J. A. & Illas, F. Atomic and electronic structure of molybdenum carbide phases: bulk and low Miller-index surfaces. *Phys. Chem. Chem. Phys.* 15, 12617–12625 (2013).
32. Ali, M., Pervaiz, E. & Rabi, O. Enhancing the overall electrocatalytic Water-Splitting efficiency of Mo2C nanoparticles by forming hybrids with UiO-66 MOF. *ACS Omega.* 6, 34219–34228 (2021).
33. Wu, S. et al. Molybdenum carbide nanoparticles assembling in diverse heteroatoms doped carbon matrix as efficient hydrogen evolution electrocatalysts in acidic and alkaline medium. *Carbon N Y.* 171, 385–394 (2021).
34. Fan, J. et al. β-Mo_2 C nanoparticles produced by carburization of molybdenum oxides with carbon black under microwave irradiation for electrocatalytic hydrogen evolution reaction. *ACS Appl. Nano Mater.* 4, 12270–12277 (2021).
35. Yang, X. et al. Facet-tunable coral-like Mo2C catalyst for electrocatalytic hydrogen evolution reaction. *Chem. Eng. J.* 451, 138977 (2023).
36. Lv, C. et al. Ultrafast synthesis of molybdenum carbide nanoparticles for efficient hydrogen generation. *J. Mater. Chem. A.* 5, 22805–22812 (2017).
37. Wu, H. B., Xia, B. Y., Yu, L., Yu, X. Y. & Lou, X. W. D. Porous molybdenum carbide nano-octahedrons synthesized via confined carburization in metal-organic frameworks for efficient hydrogen production. *Nat. Commun.* 6, 6512 (2015).
38. Shinagawa, T., Garcia-Esparza, A. T. & Takanabe, K. Insight on Tafel slopes from a microkinetic analysis of aqueous electrocatalysis for energy conversion. *Sci. Rep.* 5, 13801 (2015).
39. Ferriday, T. B., Middleton, P. H. & Kolhe, M. L. Review of the hydrogen evolution reaction—a basic approach. *Energies* 14, 8535 (2021).
40. Parsons, R. General equations for the kinetics of electrode processes. *Trans. Faraday Soc.* 47, 1332 (1951).
41. Exner, K. S., Sohrabnejad-Eskan, I. & Over, H. A universal approach to determine the free energy diagram of an electrocatalytic reaction. *ACS Catal.* 8, 1864–1879 (2018).
42. Kibsgaard, J. & Chorkendorff, I. Considerations for the scaling-up of water splitting catalysts. *Nat. Energy.* 4, 430–433 (2019).
43. Hankin, A., Bedoya-Lora, F. E., Alexander, J. C., Regoutz, A. & Kelsall, G. H. Flat band potential determination: avoiding the pitfalls. *J. Mater. Chem. A.* 7, 26162–26176 (2019).
44. Wang, Y. et al. Thermoelectric properties of moc monolayers from first-principles calculations. *AIP Adv* 10, 125220 (2020).
45. Melitz, W., Shen, J., Kummel, A. C. & Lee, S. Kelvin probe force microscopy and its application. *Surf. Sci. Rep.* 66, 1–27 (2011).
46. Anantharaj, S. et al. Precision and correctness in the evaluation of electrocatalytic water splitting: revisiting activity parameters with a critical assessment. *Energy Environ. Sci.* 11, 744–771 (2018).

Acknowledgements

This work has been partially funded by European Union (Next Generation, EU), through the MUR-PNRR project PRIN IMAGE (No. P2022KACL7). The authors thank the Bio-nanotech Research and Innovation Tower (BRIT) laboratory of the University of Catania (No. PONa3_00136 financed by the MIUR) for the Smartlab diffractometer facility and the PHI Versa Probe XPS facility, thus Professor G. Malandrino (University of Catania) for discussion and experimental XRD analysis and Prof. G. G. Condorelli (University of Catania) for XPS measurements provided. The authors acknowledge F. Ursino per Raman spectrum acquisition. ICN2 acknowledges funding from Generalitat de Catalunya 2021SGR00457. This study is part of the Advanced Materials programme and was supported by MCIN with funding from European Union NextGenerationEU (PRTR-C17.I1) and by Generalitat de Catalunya (In-CAEM Project). The authors thank support from the project AMaDE (PID2023-149158OB-C43), funded by MCIN/ AEI/10.13039/501100011033/ and by "ERDF A way of making Europe", by the "European Union". ICN2 is supported by the Severo Ochoa program from Spanish MCIN / AEI (Grant No.: CEX2021-001214-S) and is funded by the CERCA Programme / Generalitat de Catalunya. Part of the present work has been performed in the framework of Universitat Autònoma de Barcelona Materials Science PhD program. Funded by the Horizon Europe call HORIZON-INFRA-2021-SERV-01 project ReMade@ARI under grant agreement number 101058414. ICN2 is founding member of e-DREAM.

Author contributions

V.I., F.R. and S.M. conceived the project. V.I. performed samples fabrication and characterization, data analysis and wrote the manuscript. H.R, M.S., J.A. conducted and analyzed TEM measurements. C.LP. conducted the KPFM characterization. L.P. analyzed the XPS data acquired, thus the obtained deconvolution. All authors reviewed and commented on the manuscript at all stages.

Declarations

Competing interests
The authors declare no competing interests.

Additional information
Supplementary Information The online version contains supplementary material available at https://doi.org/10.1038/s41598-025-13853-z.

Correspondence and requests for materials should be addressed to S.M.

Reprints and permissions information is available at www.nature.com/reprints.

Publisher's note Springer Nature remains neutral with regard to jurisdictional claims in published maps and institutional affiliations.

Commissione europea

VIES

Sistema elettronico di scambio di dati sull'IVA (VIES): Verifica della validità di una partita IVA

Per verificare la validità di una partita IVA in un determinato paese / Irlanda del Nord, scegliere dall'apposito menu lo Stato membro / Irlanda del Nord in cui la verifica deve essere effettuata e inserire la partita IVA da verificare.

Sì, partita IVA valida

Stato membro / Irlanda del Nord	DE
Partita IVA	209719094
Orario di ricezione della richiesta	20/10/2025 10:31:25
Nome	---
Indirizzo	---
Numero di Consultazione	WAPIAAAAZoAvplGh

Back

v7.2.1